Feasibility Study of a High-Flow Air-Cooled Metal-Tip Microwave Thermal Ablation Needle

AppliedPhys

MDPI

Article

Feasibility Study of a High-Flow Air-Cooled Metal-Tip Microwave Thermal Ablation Needle

Mattia Dimitri [1,*], Martina Ricci [1] and Guido Biffi Gentili [2]

[1] Dipartimento di Ingegneria Industriale, Università degli Studi di Firenze, Via di Santa Marta n.3, 50139 Firenze, Italy; martina.ricci1@unifi.it
[2] Dipartimento di Ingegneria dell'Informazione, Università degli Studi di Firenze, Via di Santa Marta n.3, 50139 Firenze, Italy; biffigentiliguido@gmail.com
* Correspondence: mattia.dimitri@unifi.it

Abstract

Microwave (MW) ablation is a minimally invasive technique used to destroy pathological tissues through localized heating generated by a needle applicator. Internally cooled applicators using water circulation have long been the standard for high-power applications; however, water cooling introduces significant mechanical complexity. This work investigates the feasibility of a novel air-cooled coaxial thermal-ablation needle operating at 2.45 GHz up to 70 W. The system uses two concentric metal tubes—an outer 14 G stainless steel shaft (OD 2.1 mm) and an inner copper capillary (OD 1 mm, ID 0.7 mm)—serving simultaneously as the MW transmission line and cooling conduit, with dry air at room temperature (25 °C) flowing at 11 L/min under 5 bar input pressure. Experimental cooling efficiency tests demonstrated 78% efficiency for the shaft section in air and 32% for the section embedded in tissue. Electromagnetic and thermal simulations predicted ablation dimensions in a non-perfused liver of 35 mm short axis with ellipticity of 0.65 for the basic applicator, improving to 0.88 with an advanced PEEK-shaft design featuring a cancelling slot. A prototype was built and tested on exvivo bovine liver, achieving input matching better than −24 dB at 2.44 GHz and ablation dimensions (average of 5 tests) of 31 mm short axis and 45 mm long axis. Results confirm the feasibility of air cooling as a simpler, safer, and lower-cost alternative to water cooling for medium-power MW ablation.

Keywords: microwave ablation; air cooling; thermalablation needle; coaxial applicator; thermal comet effect; PEEK shaft; cancelling slot; minimally invasive surgery; electromagnetic simulation; thermal simulation

Academic Editor: Alexander Zhbanov

Received: 22 April 2026
Revised: 2 June 2026
Accepted: 8 June 2026
Published: 9 June 2026

1. Introduction

The integration of advanced cooling technologies in medical devices, such as microwave ablation needles, continues to evolve [1–3], driving the need for an advancement in the state of the art of cooling and ultimately the precision of these instruments.

The proposed coaxial structure using only two concentric tubes entails that water cannot be employed as cooling fluid because the characteristic impedance of the coaxial line would be too low and the transmission losses too high. Consequently, dry air or gas must be used as the dielectric of the coaxial line, allowing a significant reduction in the transmission line losses compared to those of a thin commercial coaxial cable.

However, the feasibility study of this simple solution presents practical design challenges because Poiseuille's law, which predicts the volumetric flow rate in a cylindrical

tube with a differential pressure applied on the two ends, is not fully applicable in this case, and therefore it is necessary to resort to a numerical fluid-dynamic simulation.

In this paper, we present the feasibility study of a high-flow, air-cooled needle whose very simple coaxial structure is derived from that proposed in [4], in which the shaft is a 14 G steel tube and the inner copper capillary that constitutes the central conductor of the coaxial guiding structure has an OD of 0.6 mm in order to realize a characteristic impedance of 50 Ω. This implies an ID of only 0.3 mm, which significantly restricts the air flow.

For maximum safety and ease of use, we imposed that the input pressure of the air injected in the needle should remain lower than 0.5 MPa (5 bar), available in every operating room at the connector of the compressed medical air.

From the preliminary fluid-dynamic numerical simulations, an air flow of about 1.6 L/min is expected with an input pressure of 5 bar, which implies that, for a satisfactory reduction in shaft overheating and the thermal "comet effect" [5] due to the RF backward currents flowing on its surface, the injected air must be pre-cooled below 5 °C.

Pre-cooling of the air can be realized by employing solid-state Peltier elements and a suitable heat exchanger, resulting in an additional burden on the thermal ablation system.

For the purpose of avoiding pre-cooling of the injected air, a modified high-flow 14 G coaxial applicator was designed to greatly increase the forced air flow by up to more than 10 L/min by increasing the ID of the internal capillary to 0.7 mm and OD to 1 mm. It follows that the characteristic impedance of the transmission line reduces to 37 Ω; therefore, a terminal $\lambda/4$ impedance transformer must be introduced to match the 50 Ω output impedance of the MW generator.

Numerical electromagnetic and thermal simulations of the proposed microwave applicator have been performed under the following hypotheses: the applicator radiating section is fully immersed in non-perfused, thermally invariant liver tissue; the air cooling flow is blocked; and the ambient and initial temperature of the liver is 25 °C.

In order to minimize the heating of the needle due to the losses of its coaxial guiding structure and reduce the thermal conductivity of the metallic shaft and the comet effect, two modifications of the original structure have been made: substitution of the 14 G steel shaft with a metallized copper or aluminum PEEK tube in order to increase its electrical conductivity and reduce the thermal conductivity, and introduction of a cancelling slot [4,6] etched on the metallized layer of the shaft.

To avoid a burdensome electromagnetic thermal fluid-dynamic numerical analysis, a preliminary evaluation of the forced air cooling efficiency was carried out using a simple coaxial device which reproduces the non-radiating section of the proposed needle.

2. Materials and Methods

2.1. Applicator Design

The basic structure of the new high-flow air-cooled applicator is shown in Figure 1a. Mechanically, the device is very simple, being composed of only two concentric tubes—an outer 14 G stainless steel tube serving as the shaft and outer conductor, and an inner copper capillary (OD 1 mm, ID 0.7 mm) serving as the central conductor—constituting a low-loss coaxial cable having air as dielectric, which transmits electromagnetic (EM) energy from the needle input section to the radiating terminal section. The term "radiating section" refers to the portion of the applicator that emits non-ionizing microwave electromagnetic energy at 2.45 GHz into the surrounding tissue for localized heating, and is not related to ionizing radiation (gamma or X-rays).

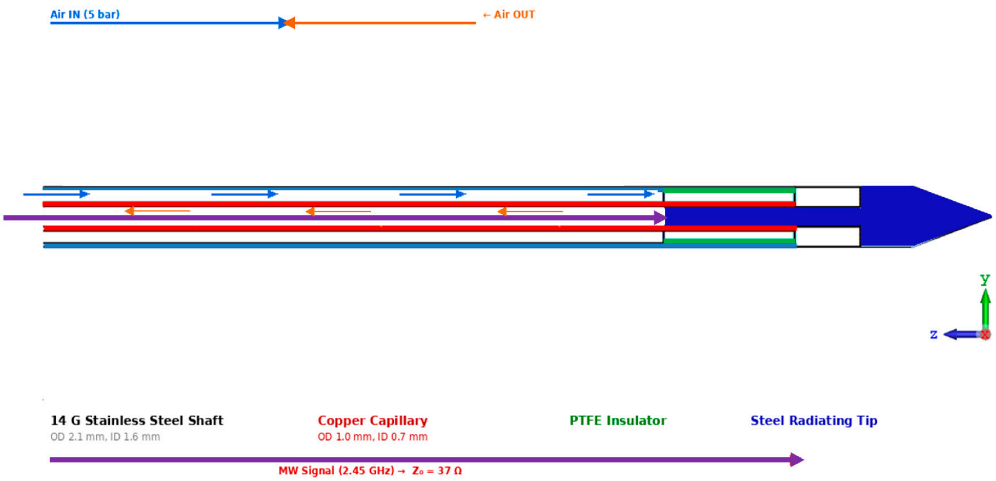

(**a**)

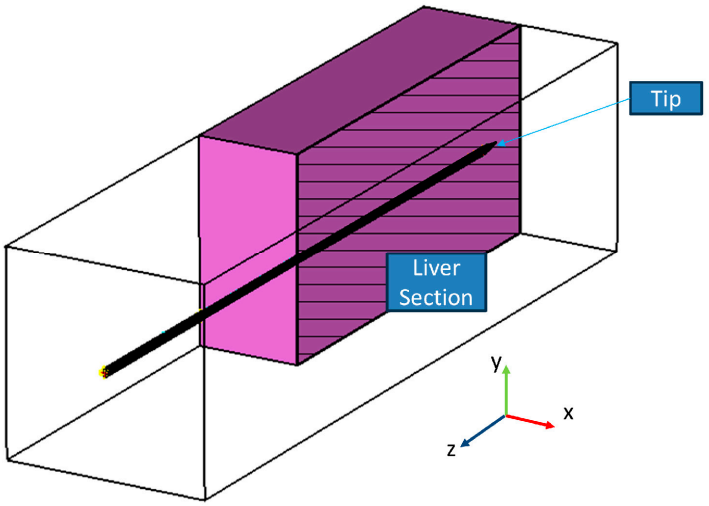

(**b**)

Figure 1. (**a**) Basic structure of the new high-flow air-cooled metal-tip microwave thermal ablation needle. The applicator consists of two concentric tubes: an outer 14 G stainless steel shaft (OD 2.1 mm, ID 1.6 mm) serving as the outer conductor, and an inner copper capillary (OD 1.0 mm, ID 0.7 mm) serving as the center conductor of a coaxial transmission line (characteristic impedance Z_0 = 37 Ω) with air as dielectric. Color coding: blue—stainless steel outer shaft; red—copper inner capillary; white—PTFE insulator and air gaps; dark blue—steel radiating tip. Blue arrows indicate the forward air flow path (Air IN at 5 bar) through the annular space; orange arrows indicate the return air flow (Air OUT) through the inner capillary. The purple arrow at the bottom indicates the MW signal propagation direction at 2.45 GHz. (**b**) Numerical analysis domain used for the electromagnetic and thermal simulations (CST Studio Suite). The 3D computational domain consists of a liver tissue block (purple volume, 6 × 6 × 9 cm) in which the applicator radiating section (Tip) is fully immersed. Absorbing Boundary Conditions (ABC) are implemented on all external walls to prevent spurious reflections. The coordinate axes (x, y, z) are indicated.

The RF signal at 2.45 GHz is injected at the proximal end of the coaxial structure through a feeding handle (Section 2.5) and propagates along the air-dielectric coaxial line. The characteristic impedance of this line is 37 Ω, matched to the 50 Ω generator output through a λ/4 impedance transformer integrated in the handle. At the distal end, the MW energy is radiated into the tissue by the metal- tip antenna section.

The cooling air at room temperature, injected at the input section into the annular space between the two coaxial tubes, flows towards the tip and, through a hole made in the internal one, reflows backwards towards the output.

A silicone gasket prevents air from escaping out of the applicator tip. The radiating section of the needle consists of a steel rod welded to the inner copper tube, covered by a cylindrical Polytetrafluoroethylene (PTFE, commercially known as Teflon) insulator and terminating in a sturdy steel radiating tip [4]. Figure 1b shows the numerical analysis domain of the applicator partially immersed in a block of biological tissue, whose walls implement the open boundary conditions.

2.2. Experimental Air Cooling Efficiency Test

This preliminary test aims to experimentally verify the air cooling efficiency of the two shaft sections of the applicator of Figure 1b, separated by the air/tissue interface. The cooling efficiency η is defined as: η = (T_without_cooling − T_with_cooling)/(T_without_cooling − T_ambient), where T_ambient = 25 °C. This metric quantifies the fraction of the maximum achievable temperature reduction.

As a practical matter, this test was performed using DC resistive (Joule-effect) heating from an external power supply (0–30 V, 0–10 A), rather than a microwave generator, to allow precise and repeatable control of the thermal power delivered to the shaft. For this purpose, a test device was realized, shown in Figure 2, which reproduces the non-radiating section of the applicator.

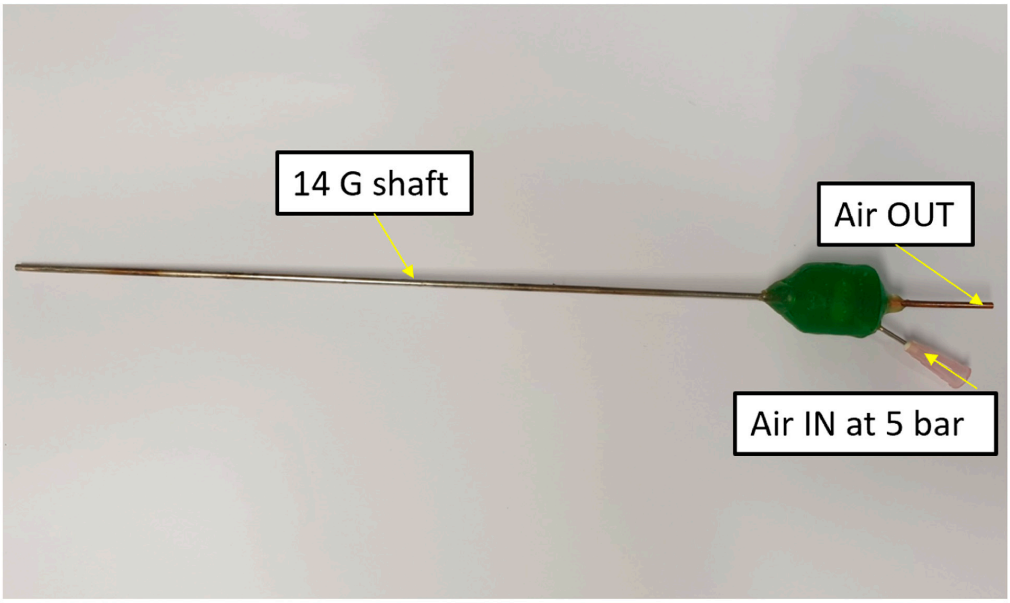

Figure 2. Air-cooled shaft device without the radiating section for testing cooling efficiency at 11 L/min air flow.

To emulate the section of the applicator operating in air during an ablation procedure, the temperature of the test device was raised to more than 100 °C with blocked air cooling, by making a strong DC current flow through the shaft from an external power supply. This resistive Joule-effect heating was adjusted to produce the same heating of the uncooled coaxial shaft when 70 W of MW power flows through it.

During the experiment, the test device temperature was measured using a thin thermocouple fixed on the middle of its external surface. Once the maximum temperature of 104 °C was reached, the cooling of the device was started by injecting air at ambient temperature (25 °C) and 5 bar input pressure, producing an 11 L/min flow rate.

To emulate the section of the applicator embedded in the biological tissue, the test device was instead immersed in a volume of 150 milliliters of pre-heated water at a temperature above 60 °C, at which near-instantaneous coagulative necrosis of tumour cells occurs [6]. The water was selected as a practical tissue-mimicking surrogate because its thermal capacity (4.18 vs. 3.6 kJ/(kg·K)), thermal conductivity (0.60 vs. 0.52 W/(m·K)), and thermal diffusivity are slightly higher than those of liver tissue [7]. It was contained in a thermostat to minimize heat dissipation towards the environment, thus emulating the insulating effect of surrounding tissue during an in vivo procedure.

2.3. Electromagnetic and Thermal Simulation

The complete coupled electromagnetic, thermal, and fluid-dynamic simulation of the applicator, partially inserted into the biological tissue, is too complex and heavy in terms of computational cost without using a cluster of computers. In order to reduce the calculation time, the following simplifications have been applied: the biological tissue (non-perfused liver) subjected to the thermal ablation process is homogeneous and isotropic with time-invariant dielectric and thermal properties; and the air inside the applicator is considered as static for the entire duration of the simulated thermal ablation process.

Under the aforementioned simplifying hypotheses, the CST Studio Suite simulator [8] was employed to calculate the power density and temperature distribution in the liver tissue during a 10 min ablation treatment, which represents a standard clinical protocol for hepatic MW ablation at this power level [9].

The electromagnetic analysis was performed using a frequency-domain solver with tetrahedral mesh refinement near the radiating tip (minimum element size 0.1 mm). The computed specific absorption rate (SAR) distribution was used as the heat source for a transient thermal solver. Liver tissue properties were set as: relative permittivity $\varepsilon' = 43.0$, effective conductivity $\sigma = 1.69$ S/m, density $\varrho = 1060$ kg/m^3, specific heat c = 3600 J/(kg·K), and thermal conductivity k = 0.52 W/(m·K), corresponding to published room-temperature properties of bovine liver tissue. The simplifying assumption of temperature-independent properties is critically discussed in Section Effect of Temperature-Dependent Dielectric Properties.

2.4. Advanced Applicator Design with Cancelling Slot

To reduce the electromagnetic and thermal tail which produce the comet effect and increase the ablation sphericity, a modified applicator was conceived where the steel shaft is replaced by a PEEK (Poly Ether Ether Ketone) tube of the same OD diameter, metallized with a thin layer of copper or aluminum. PEEK was selected because its thermal conductivity (0.25 W/(m·K)) is approximately 60 times lower than that of stainless steel (15 W/(m·K)), drastically reducing parasitic heat conduction along the shaft, while the metallization maintains adequate electrical conductivity for low-loss MW transmission and enables fabrication of a cancelling slot by simple etching. The thickness of the metallic layer is set to three times the skin depth (δ) of the electromagnetic wave at 2.45 GHz operating frequency: at this thickness, the field is attenuated by $e^{-3} \approx 0.05$ (95% attenuation), ensuring effective confinement of RF currents on the metallized surface while minimizing thermal conduction through the metal layer [10].

This solution allows the thermal conductivity of the shaft to be significantly reduced while increasing its electrical conductivity. Furthermore, a cancelling slot can be easily etched on the metallization layer of the PEEK tube, which constitutes a radiating source capable of cancelling the regressive RF currents propagating on the shaft surface. The complete structure of this technologically advanced applicator is illustrated in Figure 3, where the PEEK metallized shaft, the cancelling slot position, and the $\lambda/4$ impedance

transformer section are clearly identified. The cancelling slot, etched on the metallized layer at a calculated distance from the radiating tip, acts as a secondary radiating source that generates a field opposing the backward-propagating RF currents on the shaft surface.

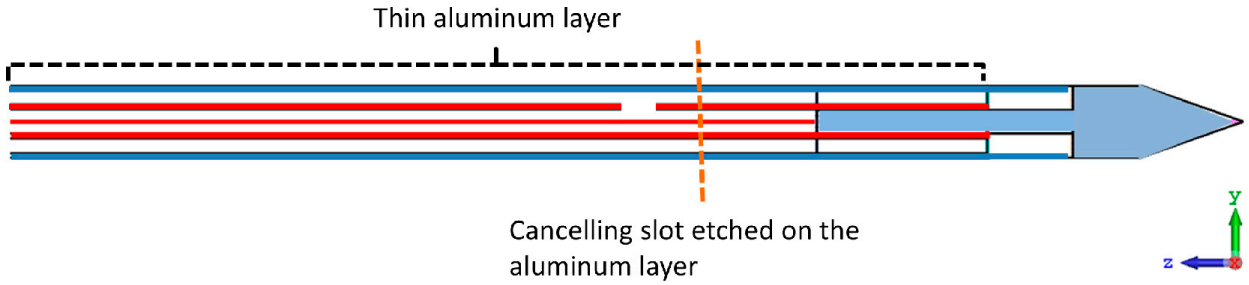

Figure 3. Technologically advanced coaxial air-cooled applicator with PEEK metallized shaft and cancelling slot. Color coding: blue—PEEK (Poly Ether Ether Ketone) shaft tube; black dashed outline—thin aluminum metallization layer deposited on the PEEK surface; red—inner copper capillary (center conductor); white—PTFE insulator and air dielectric gaps; light blue (steel-colored)—stainless steel radiating tip; orange dashed line—cancelling slot etched on the aluminum layer at a calculated distance from the radiating tip to suppress backward-propagating RF currents. The coordinate axes (y, z) are indicated at the lower right.

2.5. Prototype Construction

A basic air-cooled steel shaft applicator prototype shown in Figure 4 was realized with the aim of experimentally confirming the results of the numerical simulations.

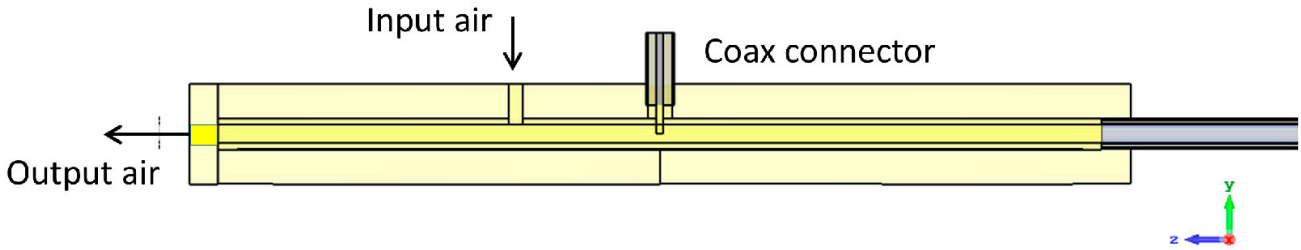

Figure 4. Prototype of the steel shaft air-cooled applicator.

A brass feeding handle, shown in Figure 5, was designed in order to: connect the applicator to the MW power source through a coaxial connector and a low-loss cable; match the 37 Ω characteristic impedance of the coaxial guiding structure to that of the MW power generator (50 Ω); and inject into the needle the cooling air coming from the terminal unit of medical compressed air available in every operating room (preferred option in clinical settings) or, for outpatient and portable applications, from a compact silent mini-compressor. The radiating tip is machined from a AISI 304 stainless steel rod and welded to the inner copper capillary (C11000 electrolytic copper). The outer shaft is a standard 14 G hypodermic tube (AISI 304L, OD 2.1 mm, wall thickness 0.25 mm). The PTFE insulator sleeve is machined from a virgin PTFE rod. All metallic components were manufactured by precision CNC machining (±0.05 mm tolerance). Assembly was performed under optical magnification to ensure coaxial alignment.

The handle integrates two $\lambda/4$ sections of a coaxial transmission line, separated by the RF input connector. The section on the right transforms the impedance from 37 to 50 Ω, while that on the left transforms into an open short-circuiting wall from which the central tube emerges. The cooling air injected in the sealed handle through a Luer Lock needle at ambient temperature (25 °C) outflows in the ambient from the central tube. The

compressed air is supplied by a compact silent mini compressor, which allows an 11 L/min air flow at output pressure of 5 bar.

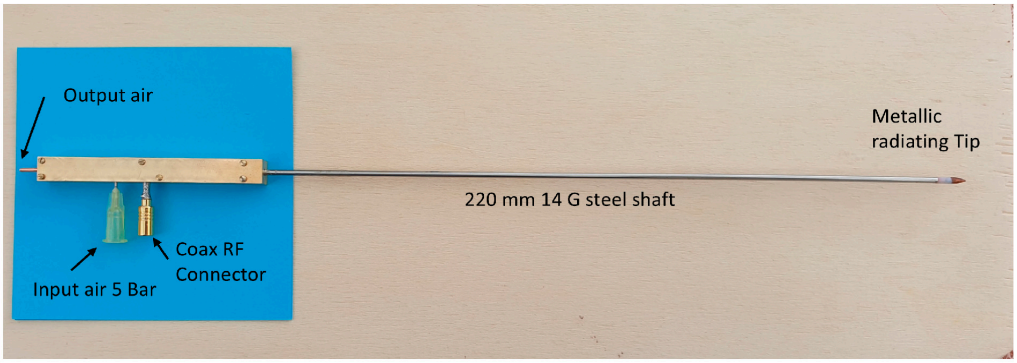

Figure 5. Handle of the air-cooled applicator.

3. Results

3.1. Air Cooling Efficiency Results

The observed temperature decrease during the shaft cooling test was approximately 60 degrees, as shown in Figure 6. A DC power supply was used to heat the shaft at 104 °C by Joule effect with blocked air cooling. With air cooling activated, the shaft temperature decreased to 40 °C.

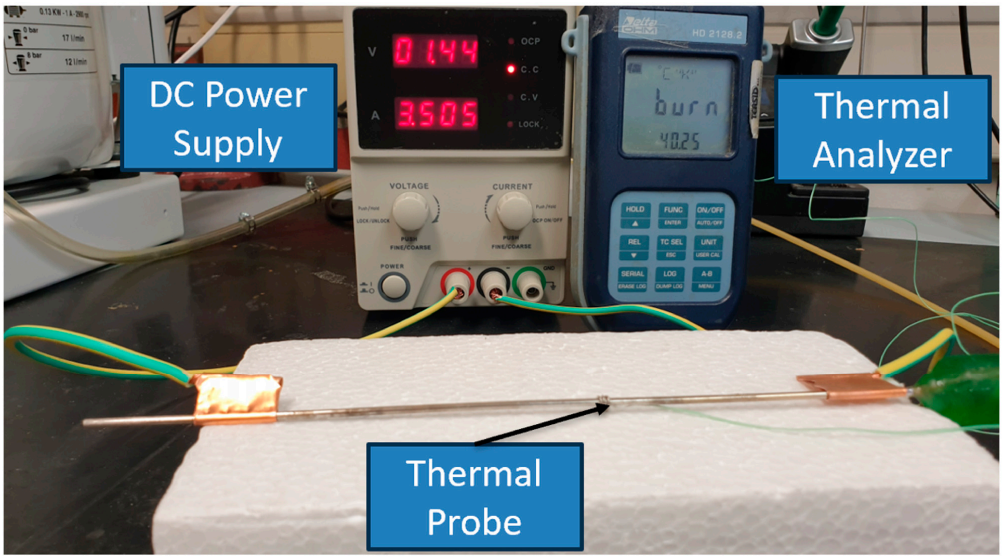

Figure 6. Shaft cooling using 11 L/min air flow at ambient temperature (25 °C). A DC power supply is used to heat the shaft at 104 °C by Joule effect, with blocked air cooling. With air cooling, the shaft temperature decreases to 40 °C.

For the test device immersed in thermostated water at 65 °C with blocked air cooling, the injection of air at 5 bar pressure and ambient temperature (25 °C), flowing at 11 L/min, caused the shaft temperature to decrease to 52 °C. Using water cooling at an ambient temperature (25 °C) flowing at 40 mL/min, the shaft temperature decreased further to 40 °C, as shown in Figure 7.

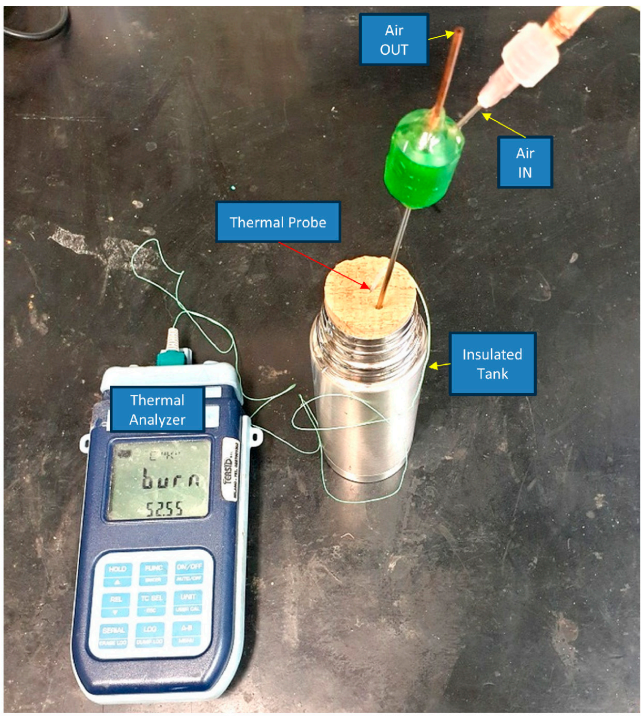

Figure 7. Shaft immersed in thermostated water at 65 °C with blocked air cooling. Air cooling at 11 L/min decreases the shaft temperature to 52 °C; water cooling at 40 mL/min decreases it to 40 °C.

We define the shaft air cooling efficiency η as:

$$\eta = (T\ without\ cooling - T\ with\ cooling)/(T\ without\ cooling - T\ Ambient) \quad (1)$$

For the shaft section operating in air, an efficiency η of 78% was obtained with a ΔP of 5 bar and an air flow of 11 L/min. For the shaft section operating inside the thermostated water at 65 °C, corresponding to that which produces the thermal comet effect in the liver tissue, an efficiency η of 32% was obtained with the same ΔP and cooling air flow.

The air flow rate of 11 L/min represents the maximum achievable flow through the coaxial needle geometry at the maximum permissible input pressure of 5 bar (the standard medical compressed air supply). Preliminary tests at reduced pressures of 3 bar and 4 bar yielded proportionally lower flow rates (approximately 7 and 9 L/min respectively) and correspondingly reduced cooling efficiencies, confirming that operation at maximum available pressure is optimal.

It was also observed that if the same testing device is cooled with standard water flowing at 40 millilit res/min, the cooling efficiency practically doubles, which is as expected because the water-to-tissue heat transfer coefficient is much greater than that of air-to-tissue.

In conclusion, by cooling with air instead of water, the comet effect is less reduced and the ellipticity of ablation increases [11]. This effect can be overcome by introducing a cancelling slot near the radiating tip which shortens both the electromagnetic and thermal tail, as shown by the following numerical simulations.

3.2. Electromagnetic and Thermal Simulation Results: Basic Applicator

Figure 8a shows the distribution of the MW power density produced by the applicator radiating into a non-perfused liver tissue. RF currents flowing backwards on the surface of the shaft cause a pronounced comet effect that extends towards the air– tissue interface.

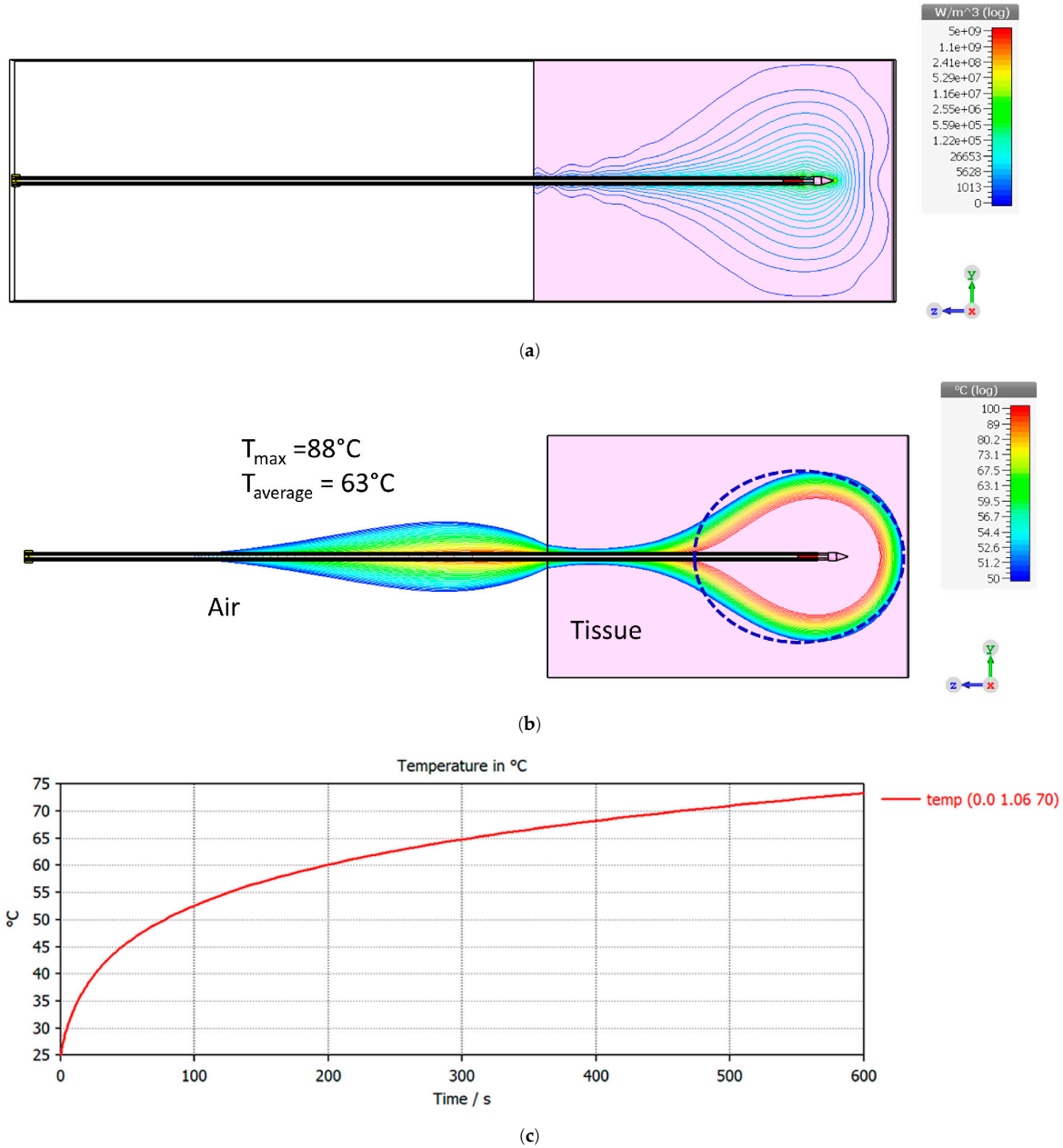

Figure 8. (**a**) EM power density distribution in the unperfused liver tissue (pink) at 2.45 GHz frequency. Liver block dimension 6 × 6 × 9 cm. (**b**) Temperature isothermals along the applicator shaft and in the liver. Ablation short axis 36 mm, long axis 55 mm, ellipticity 0.65. (**c**) Temperature increase at the air/tissue interface during 10 min treatment with Pin = 70 W and blocked air flow.

Figure 8b shows the results of the transient thermal simulation for an input power of 70 W and with a 10 min treatment. The temperature of the shaft section external to the liver tissue reaches its maximum of 88 °C near the air/tissue interface without air cooling. With air cooling, the maximum temperature will reduce to 42 °C.

Figure 8c shows the temperature increase at the air/tissue interface (needle insertion point) during the 10 min treatment with an input power of 70 W and blocked air flow, reaching approximately 88 °C. When air cooling is activated, this temperature is expected to decrease significantly, remaining well below 50 °C to avoid skin burns at the needle insertion point, as confirmed by the experimental cooling tests of Section 3.1.

Note that the obtained temperature distribution in the liver is purely indicative because the numerical simulator does not take into account the temperature dependence of the

dielectric and thermal properties of the tissue nor the migration of liquids and vapour along the shaft, which causes a significant lengthening of the thermal tail.

The predicted final diameter of the ablation is just under 35 mm for 42 kJ of energy released to the tissue, approximately 10% of which is attributed to the thermal tail and to the heat conduction of the shaft and surrounding tissues.

3.3. Electromagnetic and Thermal Simulation Results: Advanced Applicator

Figure 9a shows the distribution of the MW power density produced by the new applicator radiating into liver tissue in the absence of blood perfusion. Compared with the results of Figure 8a, a drastic reduction in the electromagnetic comet effect is evidenced.

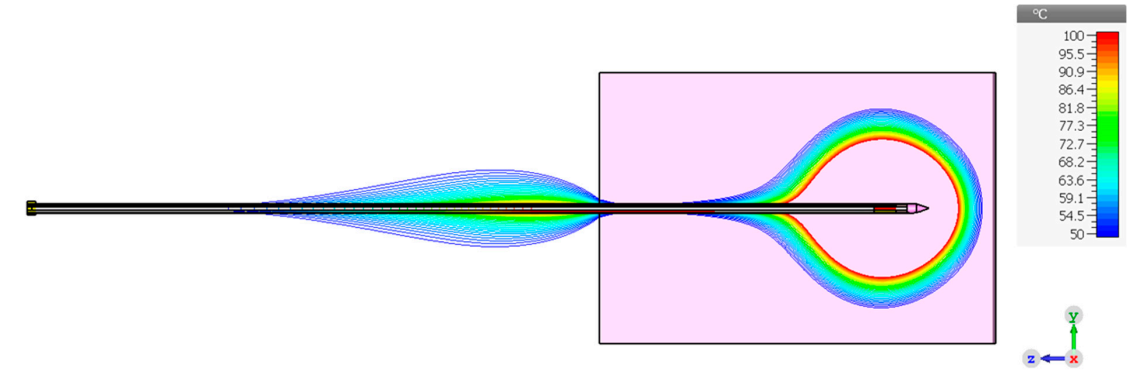

(**a**)

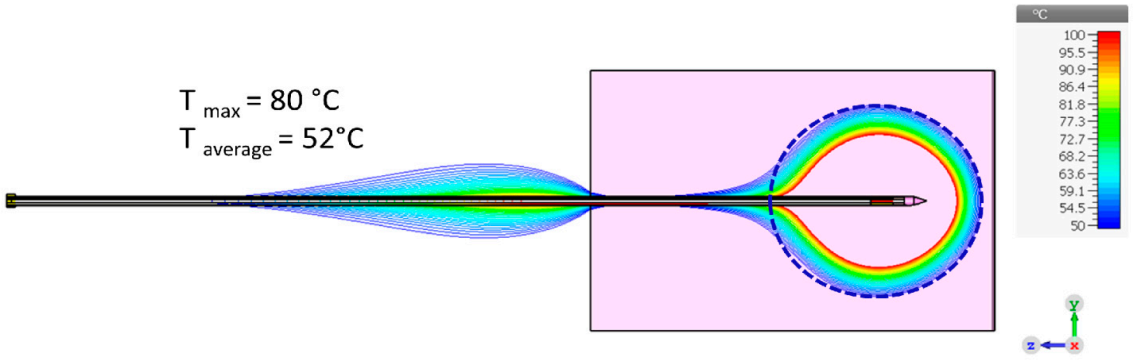

(**b**)

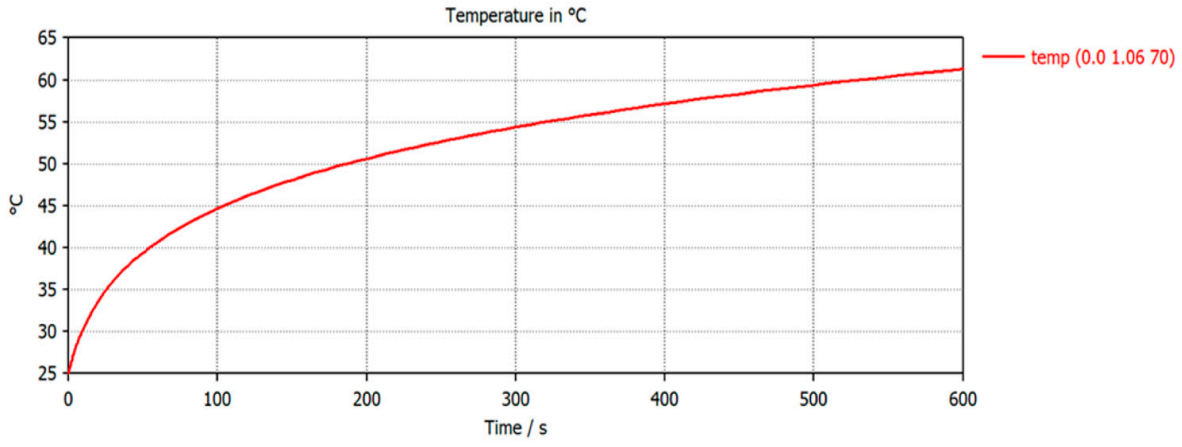

(**c**)

Figure 9. (**a**) EM power density distribution in the unperfused liver tissue (pink) at 2.45 GHz frequency. Liver block dimension 6 × 6 × 9 cm. (**b**) Temperature isothermals along the applicator shaft and in the liver. Ablation short axis 37 mm, long axis 42 mm, ellipticity 0.88. (**c**) Temperature increase at the air/tissue interface during 10 min treatment with Pin = 70 W and blocked air flow.

Figure 9b shows the results of the transient thermal simulation for an input power of 70 W and under a 10 min treatment. The temperature of the shaft section external to the liver tissue reaches its maximum of 80 °C near the air/tissue interface without air cooling. With air cooling, the maximum temperature will reduce to less than 40 °C.

It is worth noting that the shortening of the electromagnetic tail translates into a lower ellipticity of the thermal ablation and a small increment in its transverse diameter [11].

Figure 9c shows the temperature increase during a 10 min treatment with an input power of 70 W in correspondence with the needle insertion point, which will decrease strongly by activating the air cooling.

3.4. Prototype Experimental Results

The radiating section of the needle was inserted in a 6 × 6 × 10 cm^3 block of freshly extracted bovine liver obtained from a local slaughterhouse. These dimensions were chosen to substantially exceed the expected ablation zone, providing sufficient margin to avoid boundary effects on the temperature distribution. Figure 10 shows the measured applicator input matching when the radiating section is immersed in the liver tissue, demonstrating a return loss better than −24 dB at 2.44 GHz.

Figure 10. Input matching (S11 return loss) of the coaxial air-cooled applicator prototype measured with a vector network analyzer. The yellow curve represents the magnitude of the reflection coefficient S11 (in dB) as a function of frequency, from 2.000 GHz (START) to 3.000 GHz (STOP), with a vertical scale of 10 dB/division. The triangular marker (▶M1) indicates the minimum return loss of −24.85 dB at 2.440 GHz, confirming excellent impedance matching at the operating frequency.

Input matching measurements were performed using a calibrated vector network analyzer (VNA) with a full one-port SOL (Short-Open-Load) calibration at the SMA (Sub-Miniature version A) connector plane. The return loss was measured over the 2.0–3.0 GHz frequency range with the radiating section fully immersed in freshly excised bovine liver at 25 °C. The input matching remained stable (within ±0.5 dB variation) with and without air flow, confirming that air cooling does not affect the electromagnetic performance. The MW power for ablation experiments was supplied by a solid-state generator (2.45 GHz, 70 W max, 50 Ω output) connected via a low-loss coaxial cable (RG-142, insertion loss < 0.5 dB). Forward and reflected power were monitored using a dual directional coupler.

Figure 11 shows a thermal ablation produced in the ex vivo liver tissue starting from the initial ambient temperature (25 °C). The ablation dimensions measured with a calliper are: short- axis diameter 34 mm and long-axis diameter 52 mm, with an ellipticity of 0.65.

The heat-sink effect produced by a large hepatic vein is visible, as well as the elongation of the thermal tail with respect to the numerical results of Figure 5b, caused by the migration of liquids and superheated vapour along the shaft section immersed in the ex vivo liver tissue. The cooling of the shaft significantly reduces carbonization phenomena. The average ablation dimensions over five repeated experiments were: short axis 31 ± 2 mm, long axis 45 ± 4 mm, and ellipticity 0.69 ± 0.04, with standard deviations reflecting inter-sample tissue variability and vascular anatomy differences.

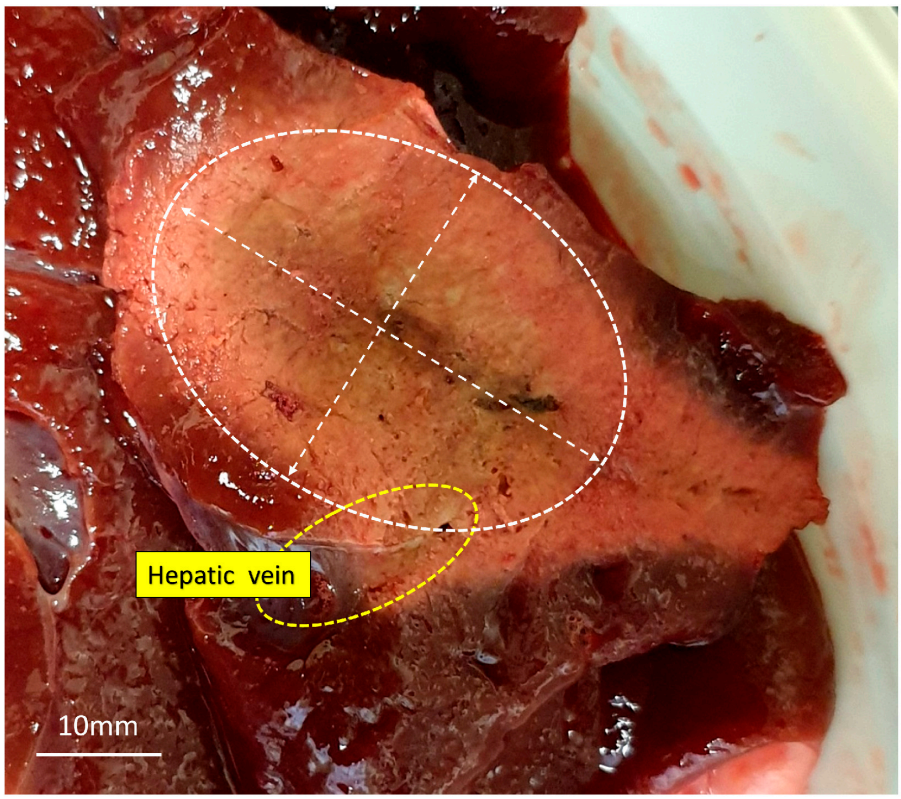

Figure 11. Liver thermal ablation with 42 kJ delivered energy. Short axis 34 mm, long axis 52 mm, ellipticity 0.65 (white ellipse). A distortion of the ablation due to the presence of a near hepatic vein is observed. The white ellipse in this image indicates the size of the area affected by the ablation.

4. Discussion

In MW ablation systems, the microwave energy serves exclusively as the heating source for tissue destruction, while a separate cooling subsystem removes excess heat from the applicator shaft. Currently, the most commonly used cooling technology for interstitial microwave ablation needles utilizes water as the cooling fluid. Another strategy for antenna cooling is the use of compressed gas, namely carbon dioxide [12]. Rapid decompression of CO_2 gas causes the Joule–Thomson phenomenon to occur at the probe tip, with venting up the shaft and along feed lines.

The high cooling capacity of this system allows the use of high-power generators while maintaining a small needle shaft diameter. However, this technology is complicated from a pneumatic point of view and expensive due to the use of special sensors and high-pressure control devices. A notable drawback of existing CO_2-based cooling systems is that they require high-pressure gas bottles (typically 60 bar), which increase equipment cost, handling complexity, and setup time in the operating room—a limitation that the proposed low-pressure air system (<5 bar) avoids entirely.

Alternatively, for medium-power microwave ablation treatments, the proposed simpler and more reliable technical approach is based on the use of low-pressure air (<10 bar) available in every operating room or generated by a small, low-cost silent compressor.

This solution still makes it necessary to redesign the applicator, taking into account that the specific heat capacity of dry air at constant pressure is four times less than that of water and the air-to-air heat transfer coefficient is much smaller than the air-to-tissue one.

The proposed designs illustrated in Figures 1a and 6, based on maximizing the air flow inside the applicator and minimizing losses in the microwave guiding structure, are mechanically simple and sturdy because they do not use fragile ceramic parts.

A prototype of the basic applicator of Figure 1a has been realized and tested, obtaining the following performances: maximum microwave input power of 70 W; ablation time of 10 min; input matching better than −20 dB; maximum temperature of the shaft section not inserted into the tissue and at the air/tissue interface of 40 °C; power efficiency better than 90%; and elliptical ablation dimensions (average of five ablations) in exvivo liver of 31 mm short axis, 45 mm long axis, ellipticity 0.69, with tail length less than 25 mm.

The observed elongation of the comet effect, due to the migration of liquids and vapour in the tissue along the shaft, could be reduced by employing the technologically advanced applicator of Figure 6, which uses an integrated cancelling slot.

The air cooling efficiency of 78% measured for the shaft section in air, while lower than the near-100% efficiency achievable with water cooling, is sufficient to maintain shaft temperatures below 40 °C at 70 W input power. For the section embedded in tissue, the efficiency of 32% (versus approximately 64% with water at 40 mL/min) results in a larger thermal tail; however, this limitation is effectively compensated by the cancelling slot of the advanced applicator, which improves the ablation ellipticity from 0.65 to 0.88.

The predicted short-axis diameter of approximately 35 mm shows good agreement with the single-test experimental measurement of 34 mm. The average over five ablation tests yielded a slightly smaller short axis of 31 mm, attributable to the natural variability of biological tissue, the heat-sink effect of blood vessels, and temperature-dependent tissue properties not accounted for in the simulation.

The advanced PEEK-shaft applicator with the cancelling slot demonstrates significant advantages over the basic steel shaft design: the electromagnetic comet effect is drastically reduced, and the ablation ellipticity improves from 0.65 to 0.88, approaching a more clinically desirable spherical zone. The main disadvantage is increased manufacturing complexity, as the PEEK tube requires precision metallization and subsequent etching of the cancelling slot.

From a clinical perspective, the elimination of water circulation removes the risk of fluid leakage into the tissue, simplifies sterilization procedures, and reduces the overall cost and setup time. While the current prototype demonstrates technical feasibility, commercialization would require further in vivo validation, biocompatibility testing, and compliance with medical device standards (IEC 60601 series [13]).

The radiating section of the applicator was designed to avoid air leaks during the thermal ablation procedure; however, any small air leakage into the tissue can be immediately detected using real-time ultrasound imaging.

Effect of Temperature-Dependent Dielectric Properties

The electromagnetic and thermal simulations presented in this work were performed assuming constant (temperature-independent) dielectric and thermal properties of liver tissue. However, the operating frequency of 2.45 GHz lies within the tail of the dielectric relaxation spectrum of water, which constitutes 70–80% of biological tissue by weight. Published experimental measurements [14,15] indicate that as liver tissue temperature

increases from 37 °C to 100 °C, the relative permittivity (ε') decreases by approximately 25% (from ~43 to ~32) and the effective conductivity (σ_eff, proportional to ε'') decreases by approximately 40% (from ~1.7 S/m to ~1.0 S/m) at 2.45 GHz. Above 100 °C, tissue desiccation and water vaporization cause further dramatic reductions in both quantities.

The decrease in effective conductivity at elevated temperatures implies reduced microwave absorption near the antenna tip, creating a self-limiting feedback mechanism: as tissue desiccates, MW energy penetrates deeper into cooler surrounding tissue, moderately broadening the ablation zone compared to constant-property predictions. This phenomenon has been documented by several authors [16,17] and represents a well-known source of discrepancy between simplified simulations and experimental observations.

In the present feasibility study, the experimental results on exvivo bovine liver (Section 3.4) inherently capture all temperature-dependent phenomena, including dielectric property changes, liquid and vapour migration, and tissue desiccation. The good agreement between simulated (~35 mm) and measured (34 mm single test) short-axis ablation diameters suggests that the constant-property simulation provides a reasonable first-order estimate of the ablation dimensions. Based on this assessment, we conclude that the temperature dependence of dielectric properties, while quantitatively significant (up to 40% change in effective conductivity), does not critically undermine the feasibility conclusions of this study, as the dominant effect is a moderate redistribution of absorbed power density that tends to enlarge rather than reduce the ablation zone. Nevertheless, the incorporation of temperature-dependent tissue models in future coupled electromagnetic–thermal– fluid-dynamic simulations is essential for accurate ablation zone prediction and clinical planning [18].

5. Conclusions

This work addressed for the first time, to the authors' knowledge, the feasibility study of a new thermal ablation needle that uses air at room temperature as a cooling fluid. The main motivations of this study were:

- Reducing the mechanical complexity of the needle and its production cost;
- Increasing applicator reliability and robustness;
- Improving applicator usability and safety;
- Reducing ablator setting time for the operators and procedure time for the patients;
- Enabling easy sterilization of the applicator for alternative use and reuse in non-oncological fields;
- Facilitating easy transformation of the applicator structure from rigid to flexible.

The experimental results demonstrated: air cooling efficiency of 78% for the shaft in air and 32% in tissue surrogate, with shaft temperature reduction from 104 °C to 40 °C; input matching better than −24 dB at 2.44 GHz; ex vivo liver ablation dimensions (average of 5 tests) of 31 mm short axis and 45 mm long axis (ellipticity 0.69) with 42 kJ delivered energy; and power efficiency above 90%.

The main limits of this work are the lack of a complex numerical simulation closer to the real environment that couples electromagnetic with thermal and fluid-dynamics modelling of the air-cooled applicator, and the lack of exhaustive experimental testing of the two proposed versions of the air-cooled ablation needle on both ex vivo and in vivo biological tissue, possibly coupled with a perfusion machine. The authors aim to address these aspects in future studies.

From the first encouraging results, the opportunity to continue the research emerges, in particular: to realize and test a technologically advanced version of the applicator of Figure 6, which should allow a significant reduction in the comet effect thanks to the introduction of a cancelling slot etched on the thin metallization of the PEEK shaft; and to

inject pre-cooled air into the applicator in order to increase the input power up to 100 W while improving the sphericity of the thermal ablation, using a special static cooler based on Peltier cell devices.

Additionally, future computational studies will incorporate temperature-dependent dielectric and thermal tissue properties, using established experimental models [14,17,18], to improve the accuracy of ablation zone predictions and enable reliable pre-operative planning.

Author Contributions: Conceptualization, M.D. and G.B.G.; methodology, M.D. and G.B.G.; software, M.D.; validation, M.D. and M.R.; formal analysis, M.D. and G.B.G.; investigation, M.D. and M.R.; resources, M.D. and G.B.G.; data curation, M.D.; writing—original draft preparation, M.D. and G.B.G.; writing—review and editing, M.D., M.R. and G.B.G.; visualization, M.D.; supervision, G.B.G.; project administration, M.D. All authors have read and agreed to the published version of the manuscript.

Funding: Financial support from the Italian Ministry of University and Research (Next Generation EU, National Recovery and Resilience Plan, Investment PE8, project "Age-It: Ageing Well in an Ageing Society", grant DM 1557 11 October 2022) is gratefully acknowledged.

Institutional Review Board Statement: Not applicable.

Informed Consent Statement: Not applicable.

Data Availability Statement: The data presented in this study are available on request from the corresponding authors.

Acknowledgments: The authors wish to thank the Department of Information Engineering of the University of Florence for providing access to the CST Studio Suite simulation facilities used in this work. The authors wish to thank the slaughterhouse "Ciccia e Pane" (via Luigi Boccherini 22, 50144 Firenze, Italy) for providing the ex-vivo tissues of bovine liver used for the experiments described in the manuscript.

Conflicts of Interest: The authors declare no conflicts of interest.

References

1. Brancadoro, M.; Dimitri, M.; Boushaki, M.N.; Staderini, F.; Sinibaldi, E.; Capineri, L.; Cianchi, F.; Biffi Gentili, G.; Menciassi, A. A novel microwave tool for robotic liver resection in minimally invasive surgery. *Minim. Invasive Ther. Allied Technol.* **2022**, *31*, 42–49. [CrossRef] [PubMed]
2. Dimitri, M.; Biffi Gentili, G.; Staderini, F.; Brancadoro, M.; Menciassi, A.; Coratti, A.; Cianchi, F.; Corvi, A.; Capineri, L. Development of a robotic surgical system of thermal ablation and microwave coagulation. In Proceedings of the 2019 PhotonIcs & Electromagnetics Research Symposium—Spring (PIERS-Spring), Rome, Italy, 17–20 June 2019.
3. Dimitri, M.; Staderini, F.; Brancadoro, M.; Frosini, F.; Coratti, A.; Capineri, L.; Corvi, A.; Cianchi, F.; Biffi Gentili, G. A new microwave applicator for laparoscopic and robotic liver resection. *Int. J. Hyperth.* **2019**, *36*, 75–86. [CrossRef] [PubMed]
4. Bertram, J.M.; Yang, D.; Converse, M.C.; Webster, J.G.; Mahvi, D.M. A review of coaxial-based interstitial antennas for hepatic microwave ablation. *Crit. Rev. Biomed. Eng.* **2006**, *34*, 187–213. [CrossRef] [PubMed]
5. Biffi Gentili, G. Applicatore per Termoablazione. Italian Patent FI2013A000268, 15 November 2013.
6. Goldberg, S.N.; Grassi, C.J.; Cardella, J.F.; Charboneau, J.W.; Dodd, G.D.; Dupuy, D.E.; Gervais, D.A.; Gillams, A.R.; Kane, R.A.; Lee, F.T.; et al. Image-guided tumor ablation: Standardization of terminology and reporting criteria. *Radiology* **2005**, *235*, 728–739. [CrossRef]
7. Wright, A.S.; Lee, F.T., Jr.; Mahvi, D.M. Hepatic microwave ablation with multiple antennae results in synergistically larger zones of coagulation necrosis. *Ann. Surg. Oncol.* **2003**, *10*, 275–283. [CrossRef] [PubMed]
8. Li, Y.; Wu, W.; Li, Y.; Li, J.; Sun, M. Efficacy and safety of endovenous microwave ablation versus laser ablation for great saphenous vein varicosis: Study protocol for a multicentre, randomised controlled non-inferiority trial. *BMJ Open* **2022**, *12*, e059213. [CrossRef] [PubMed]
9. Hope, W.W.; Schmelzer, T.M.; Newcomb, W.L.; Heath, J.J.; Lincourt, A.E.; Norton, H.J.; Heniford, B.T.; Iannitti, D.A. Guidelines for power and time variables for microwave ablation in an in vivo porcine kidney. *J. Surg. Res.* **2009**, *153*, 263–267. [CrossRef] [PubMed]
10. Pozar, D.M. *Microwave Engineering*, 4th ed.; Wiley: Hoboken, NJ, USA, 2012.

11. Bucky, L.P. Microwave-assisted lipoplasty: A new treatment for body contouring. *Aesthet. Surg. J.* **2000**, *20*, 439–440. [CrossRef]
12. Knavel, E.M.; Hinshaw, J.L.; Lubner, M.G.; Andreano, A.; Warner, T.F.; Lee, F.T.; Brace, C.L. High-powered gas-cooled microwave ablation: Shaft cooling creates an effective stick function without altering the ablation zone. *AJR Am. J. Roentgenol.* **2012**, *198*, W260–W265. [CrossRef] [PubMed]
13. *IEC 60601-1*; Medical Electrical Equipment—Part 1: General Requirements for Basic Safety and Essential Performance. International Electrotechnical Commission (IEC): Geneva, Switzerland, 2020.
14. Lazebnik, M.; Converse, M.C.; Booske, J.H.; Hagness, S.C. Dielectric properties of ex vivo liver tissue from 0.5 to 20 GHz measured with an open-ended coaxial probe. *Phys. Med. Biol.* **2006**, *51*, N261–N269.
15. Gabriel, S.; Lau, R.W.; Gabriel, C. The dielectric properties of biological tissues: III. Parametric models for the dielectric spectrum of tissues. *Phys. Med. Biol.* **1996**, *41*, 2271–2293. [CrossRef]
16. Brace, C.L. Microwave tissue ablation: Biophysics, technology, and applications. *Crit. Rev. Biomed. Eng.* **2010**, *38*, 65–78. [CrossRef]
17. Lopresto, V.; Pinto, R.; Lovisolo, G.A.; Cavagnaro, M. Changes in the dielectric properties of ex vivo bovine liver during microwave thermal ablation at 2.45 GHz. *Phys. Med. Biol.* **2012**, *57*, 2309–2327. [CrossRef] [PubMed]
18. Ji, Z.; Brace, C.L. Expanded modeling of temperature-dependent dielectric properties for microwave thermal ablation. *Phys. Med. Biol.* **2011**, *56*, 5249–5264. [CrossRef] [PubMed]